BAREKENG: Journal of Mathematics and Its Applications
September 2026 Volume 20 Issue 3 Page 2549-2560
P-ISSN: 1978-7227 E-ISSN: 2615-3017
https://doi.org/10.30598/barekengvol20iss3pp2549-2560

AG-FE_3O_4 HYBRID NANOFLUID DYNAMICS: EXPLORING SLIP AND MAGNETIC EFFECTS ON THE FLOW OVER EXPONENTIALLY ELONGATED/CONTRACTED SURFACE

Rahimah Jusoh[1*], **Zulkhibri Ismail**[2], **Mikhail Sheremet**[3], **Nooraini Zainuddin**[4], **Mohd Hisyam Ariff**[5]

[1,2]*Centre for Mathematical Sciences, Universiti Malaysia Pahang Al-Sultan Abdullah Kuantan, Pahang, 26300, Malaysia.*

[3]*Laboratory of Convective Heat and Mass Transfer, Tomsk State University Tomsk, 634050, Russia.*

[4]*Department of Applied Science, Universiti Teknologi PETRONAS Bandar Seri Iskandar, Perak, 32610, Malaysia.*

[5]*Faculty of Electrical & Electronics Engineering Technology, Universiti Malaysia Pahang Al-Sultan Abdullah Pekan, Pahang, 26600, Malaysia.*

*Corresponding author's e-mail: * **rahimahj@umpsa.edu.my***

Article Info

Article History:

Received: 11th September 2025
Revised: 3rd November 2025
Accepted: 17th March 2026
Published: 8th April 2026

Keywords:

Boundary Layer Flow;
Dual Solutions;
Hybrid Nanofluid;
Magnetic Field;
Velocity Slip.

ABSTRACT

This study explores the unique advantages of hybrid nanofluids, known for their exceptional ability to boost heat transfer efficiency, making them ideal for advanced thermal applications. The objective is to assess the impact of slip and magnetic field on the velocity and temperature profiles over an exponentially elongated/contracted surface. Through the application of an appropriate similarity transformation, the governing equations for energy, momentum, and mass are converted into ordinary differential equations. These resulting equations are subsequently solved numerically via the bvp4c function in MATLAB. Results imply that magnetic fields decelerate the fluid while thickening the thermal boundary layer due to the Lorentz force. Increased viscous dissipation elevates temperature levels, while surface elongation promotes convective heat transfer. In contrast, surface contraction and velocity slip suppresses thermal transport by limiting momentum exchange. Thermal slip further reduces surface heat flux These findings underscore both the novelty and practical potential of Ag–Fe_3O_4 hybrid nanofluids in enhancing performance across thermal regulation systems, such as energy-efficient cooling devices, biomedical heat exchangers, and industrial applications.

How to cite this article:

R. Jusoh, Z. Ismail, M. Sheremet, N. Zainuddin and M. H. Ariff., "AG-FE3O4 HYBRID NANOFLUID DYNAMICS: EXPLORING SLIP AND MAGNETIC EFFECTS ON THE FLOW OVER EXPONENTIALLY ELONGATED/CONTRACTED SURFACE", *BAREKENG: J. Math. & App.*, vol. 20, no. 3, pp. 2549-2560, Sep, 2026.

Journal homepage: *https://ojs3.unpatti.ac.id/index.php/barekeng/*
Journal e-mail: *barekeng.math@yahoo.com; barekeng.journal@mail.unpatti.ac.id*

Research Article · Open Access

1. INTRODUCTION

The evolution of heat transfer fluids has progressed from conventional fluids to advanced nanofluids and, more recently, to hybrid nanofluids, driven by the need for enhanced thermal performance in engineering applications. Traditional heat transfer fluids such as water, ethylene glycol, and engine oil have limited thermal conductivity, limiting their efficiency in cooling and heat-exchange systems. The introduction of nanofluids, pioneered by Choi and Eastman [1], revolutionized thermal management by incorporating nanoparticles into base fluids. By dispersing single nanoparticles such as silica (SiO_2), copper (Cu), silver/argentum (Ag), aluminium oxide (Al_2O_3), and titanium dioxide (TiO_2), nanofluids significantly enhance heat transfer capabilities. Recognised for its outstanding heat and electrical transport properties, as well as its antimicrobial efficiency, the Ag nanofluid is extensively utilized in high- performance systems like solar collectors and additive-manufactured electronics, making it an appropriate focus for this research [2]. Experimental findings by Heravi et al. [3] suggest that integrating Fe_3O_4 nanoparticles into water can increase cooling tower efficiency by approximately 50%, a result attributed to the nanofluid's elevated thermal conductivity.

Nevertheless, to further enhance thermal performance, researchers have recently shifted towards hybrid nanofluids, which incorporate two or more types of nanoparticles, leveraging their combined thermal, electrical, and mechanical advantages [4], [5], [6]. Hybrid nanofluids were first introduced by Turcu et al. [7], marking a new frontier in nanofluid research. This transition from conventional fluids to hybrid nanofluids highlights the ongoing quest for more efficient and sustainable thermal solutions in various industries, including automotive cooling, electronics, biomedical applications, and renewable energy systems [8], [9]. Experimentally, Madhesh and Kalaiselvam [10] demonstrated that hybrid nanofluids, specifically copper-titanium hybrid nanocomposites dispersed in water, exhibited a 48.4% increase in convective heat transfer coefficient at an optimal concentration of 0.7%, highlighting their superior thermal performance as a coolant compared to conventional fluids. Utilising numerical analysis, Hyder et al. [11] demonstrated that hybrid nanofluids containing alumina oxide and Cu nanoparticles exhibit enhanced heat transfer efficiency compared to regular nanofluids, particularly in magnetohydrodynamic and thermal radiation-influenced environments, making them highly suitable for industrial applications such as casting and welding.

Slip boundary conditions play a crucial role in micro- and nanoscale fluid flows, where the conventional no-slip condition may not be valid. In particular, slip effects become significant in applications involving thin films, porous media, and biomedical flows [12]. Incorporating slip conditions in hybrid nanofluid studies allows for a more realistic representation of practical engineering scenarios, where surface roughness and interfacial interactions affect flow behaviour. Incorporating velocity slip in hybrid nanofluid flow alters the velocity and thermal boundary layers by enhancing the velocity profile, reducing skin friction on a shrinking surface while increasing it on a stretching surface, and lowering the Nusselt number, thereby diminishing heat transfer efficiency [13]. Then, Patil et al. [14] proved that the consideration of velocity slip significantly amends flow behaviour, leading to a 396% reduction in velocity magnitude and a 159% decrease in heat transfer rate, emphasising its crucial role in modulating velocity profiles and thermal transport efficiency in hybrid nanofluids. Additionally, the exponential stretching or contracting of a surface introduces complex flow characteristics that influence velocity and temperature distributions, necessitating a thorough investigation into the impact of such variations on hybrid nanofluid dynamics.

The presence of an external magnetic field further complicates the flow behaviour due to the magnetohydrodynamic (MHD) effect, which induces Lorentz forces that influence the motion of electrically conducting fluids. Magnetic nanoparticles, such as Fe_3O_4, exhibit strong responses to external magnetic fields, making them useful for applications such as targeted drug delivery, electromagnetic cooling, and ferrofluid-based lubrication [15], [16], [17]. Naseem and Kasana [18] explored the magnetic impact on the hybrid nanofluid flow and concluded that the drag force is augmented due to the increase in the skin friction factor, which occurs when the magnetic parameter escalates.

In addition to MHD and slip effects, viscous dissipation significantly alters the thermal energy distribution within the fluid flow. Viscous dissipation refers to the internal conversion of mechanical energy into heat due to viscous forces within the fluid, which becomes particularly important in high-speed and high-viscosity flows [19]. This phenomenon significantly influences the temperature field, leading to an increase in thermal energy, which can enhance or hinder heat transfer depending on the fluid properties and boundary conditions. A thorough understanding of viscous dissipation in hybrid nanofluids is imperative for achieving efficiency in industrial heat applications, lubrication frameworks, and thermal energy handling. The findings

of Waini et al. [20] indicated that viscous dissipation contributed to a 14.39% decline in heat transfer efficiency in hybrid nanofluids exhibiting power-law velocity. Then, Padma et al. [21] discovered that elevated viscous dissipation levels result in a higher temperature profile due to the influence of internal energy dissipation. Considering this effect allows for a more comprehensive understanding of the heat transfer mechanisms and provides insights into optimising cooling and heating processes in advanced engineering systems.

Among the commonly studied hybrid nanofluids, the combination of argentum and magnetite (Fe_3O_4) nanoparticles has shown promising results due to their excellent thermal conductivity and magnetic properties. In contrast to existing studies that primarily focus on linear stretching surfaces, or unsteady configurations, the present work investigates Ag–Fe_3O_4 hybrid nanofluid flow over an exponentially elongated or contracted surface, accounting for MHD, slip, and viscous dissipation effects. The governing equations are formulated to account for MHD effects, slip boundary conditions, thermal effects, and viscous dissipation, and are solved using appropriate numerical techniques. The interaction between MHD and slip conditions in hybrid nanofluids over an exponentially elongated or contracted surface has not been extensively explored, highlighting a crucial research gap. Understanding the interplay between these factors is essential for optimising the design and control of fluid transport processes in advanced engineering applications. The findings of this research contribute to the development of efficient heat transfer systems and microfluidic devices where slip, MHD, and viscous dissipation effects play a crucial role.

2. RESEARCH METHODS

The boundary layer represents the narrow region adjacent to a surface where strong gradients in velocity and temperature develop, controlled primarily by the governing equations of continuity, momentum, and energy. The basic equations of boundary layer flow are derived from the Navier–Stokes equations, which are simplified under boundary-layer assumptions. In this study, a steady two-dimensional flow of hybrid nanofluid containing Ag and Fe_3O_4 nanoparticles is scrutinised. The fundamental equations describing boundary layer continuity, momentum, and energy are expressed as follows [13]:

$$\frac{\partial u}{\partial x}+\frac{\partial v}{\partial y}=0, \tag{1}$$

$$u\frac{\partial u}{\partial x}+v\frac{\partial u}{\partial y}=\frac{\mu_{hnf}}{\rho_{hnf}}\frac{\partial^2 u}{\partial y^2}-\frac{\sigma_{hnf}B^2}{\rho_{hnf}}u, \tag{2}$$

$$u\frac{\partial T}{\partial x}+v\frac{\partial T}{\partial y}=\frac{k_{hnf}}{\left(\rho C_p\right)_{hnf}}\frac{\partial^2 T}{\partial y^2}-\frac{\mu_{hnf}}{\left(\rho C_p\right)_{hnf}}\left(\frac{\partial u}{\partial y}\right)^2. \tag{3}$$

In this context, the velocity components in the x- and y-axes are given by u and v, respectively, whereas T represents the temperature function. Moreover, the terms μ_{hnf}, $\left(\rho C_p\right)_{hnf}$, σ_{hnf}, ρ_{hnf}, and k_{hnf} characterize the hybrid nanofluid's dynamic viscosity, heat capacity, electrical conductivity, density and thermal conductivity, respectively. The problem is modelled physically in Fig. 1, below:

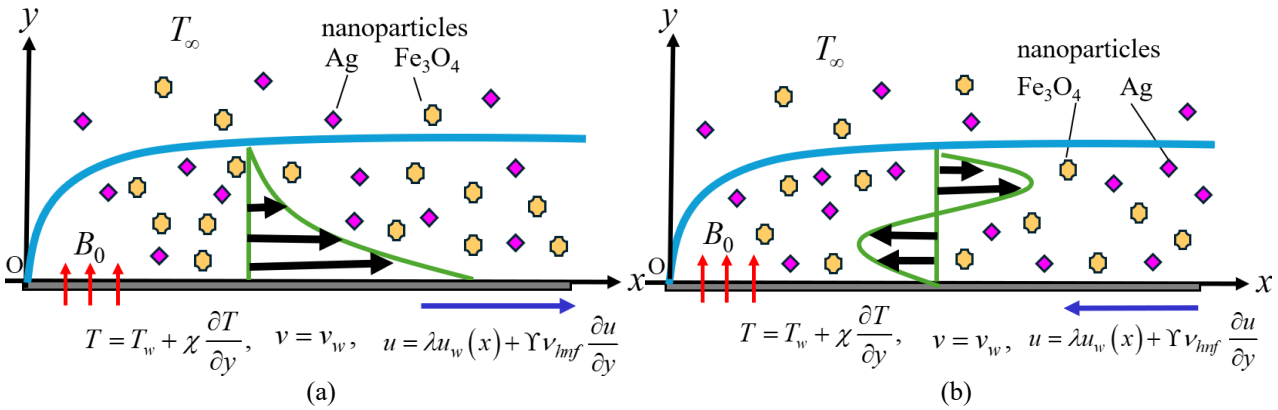

Figure 1. The Physical Configuration of Hybrid Nanofluid Flow Over an Exponentially (a) Elongated Surface, (b) Contracted Surface

The surface is considered exponentially elongated/contracted with the surface velocities $u_w = ae^{x/L}$ and $v_w = v_0 e^{x/2L}$ in x-direction and y-direction, respectively. In this context, a represents a constant with the velocity dimension, while L denotes the characteristic length. Meanwhile, $v_0 = -\sqrt{av_f/2L}s$ is a constant that corresponds to the mass flux velocity. In addition, a magnetic field, expressed as $B = B_0 e^{x/2L}$, is introduced in a direction perpendicular to the surface. In this formula, B_0 is the constant magnetic field [22].

Consideration of velocity and thermal slips in the boundary equations are given as

$$u = \lambda u_w(x) + \Upsilon v_{hnf}\frac{\partial u}{\partial y}, \qquad v = v_w, \qquad T = T_w + \chi\frac{\partial T}{\partial y} \quad \text{at} \quad y = 0,$$
$$u \longrightarrow 0, \quad T \longrightarrow T_\infty, \quad as \quad y \longrightarrow \infty, \tag{4}$$

where Υ is the velocity slip factor and χ is the thermal slip factor [13]. The formulation of the wall temperature follows $T_w = T_\infty + Te^{cx/2L}$, in which T_0 stands for the reference temperature, while c characterises the temperature exponent parameter. The following expressions define the governing similarity transformations [13]:

$$u = ae^{x/L}f'(\eta), \quad v = -\sqrt{\frac{av_f}{2L}}e^{\frac{x}{2L}}\left(f(\eta) + \eta f'(\eta)\right), \quad \theta(\eta) = \frac{T - T_\infty}{T_w - T_\infty}, \quad \eta = y\sqrt{\frac{a}{2v_f L}}e^{\frac{x}{2L}}. \tag{5}$$

As a result, Eq. (1) is naturally satisfied, leading to the transformation of Eqs. (2) – (4) into the following system of ordinary differential equations:

$$\frac{\mu_{hnf}/\mu_f}{\rho_{hnf}/\rho_f}f''' + ff'' - 2f'^2 - \frac{\frac{\sigma_{hnf}}{\sigma_f}}{\frac{\rho_{hnf}}{\rho_f}}Mf' = 0, \tag{6}$$

$$\frac{1}{\Pr}\frac{k_{hnf}/k_f}{(\rho C_p)_{hnf}/(\rho C_p)_f}\theta'' - cf'\theta + f\theta' + \frac{\frac{\mu_{hnf}}{\mu_f}}{\frac{(\rho C_p)_{hnf}}{(\rho C_p)_f}}Ecf''^2 = 0, \tag{7}$$

with the boundary conditions

$$f(0) = s, \qquad f'(0) = \lambda + \Upsilon_1 f''(0), \quad \theta(0) = 1 + \chi_1\theta'(0),$$
$$f'(\eta) \longrightarrow 0, \quad \theta(\eta) \longrightarrow 0, \quad as \quad \eta \longrightarrow \infty. \tag{8}$$

Here, Υ_1 and χ_1 represent the dimensionless velocity slip and dimensionless thermal slip, respectively. Additionally, s is the suction parameter, Pr symbolises the Prandtl number, M is the magnetic parameter and Ec is the Eckert number. All of these parameters are formulated as

$$\Upsilon_1 = \Upsilon\frac{\mu_{hnf}}{\rho_{hnf}}e^{\frac{x}{2L}}\sqrt{\frac{a}{2v_f L}}, \qquad \chi_1 = \chi e^{\frac{x}{2L}}\sqrt{\frac{a}{2v_f L}}, \qquad s = -\frac{v_0}{\sqrt{av_f/2L}}, \qquad Pr = \frac{v_f(\rho C_p)_f}{k_f},$$
$$M = \frac{2L\sigma_f {B_0}^2}{a\rho_f}, \quad Ec = \frac{{u_w}^2}{(C_p)_f(T_w - T_\infty)}. \tag{9}$$

Based on physical assumptions and practical correlations, the volume concentration of argentum and magnetite follows the equation $\phi_{hnf} = \phi_1 + \phi_2$. The hybrid nanofluid characteristics are outlined in Table 1, where subscript $s2$ refers to magnetite nanoparticles, and $s1$ corresponds to argentum nanoparticles. The base fluid, water (H_2O), is represented by f, while nf and hnf denote the nanofluid and hybrid nanofluid, respectively. For convenience, the thermophysical properties of water, argentum, and magnetite nanoparticles are provided in Table 2.

Table 1. Hybrid Nanofluid Characteristics Formulations [23], [24]

Properties	Nanofluid	Hybrid nanofluid
Density	$\rho_{nf} = (1-\phi_1)\rho_f + \phi_1\rho_s$	$\rho_{hnf} = (1-\phi_{hnf})\rho_f + \phi_1\rho_{s1} + +\phi_2\rho_{s2}$
Heat capacity	$(\rho C_p)_{nf} = (1-\phi_1)(\rho C_p)_f + \phi_1(\rho C_p)_s$	$(\rho C_p)_{hnf} = (1-\phi_{hnf})(\rho C_p)_f + \phi_1(\rho C_p)_{s1} + \phi_2(\rho C_p)_{s2}$
Dynamic viscosity	$\mu_{nf} = \frac{\mu_f}{(1-\phi_1)^{2.5}}$	$\frac{\mu_{hnf}}{\mu_f} = \frac{1}{(1-\phi_{hnf})^{2.5}}$
Thermal Conductivity	$\frac{k_{nf}}{k_f} = \frac{k_s + 2k_f - 2\phi_1(k_f - k_s)}{k_s + 2k_f + \phi_1(k_f - k_s)}$	$\frac{k_{hnf}}{k_f} = \frac{\left(\frac{\phi_1 k_{s1} + \phi_2 k_{s2}}{\phi_{hnf}}\right) + 2k_f + 2(\phi_1 k_{s1} + \phi_2 k_{s2}) - 2\phi_{hnf}}{\left(\frac{\phi_1 k_{s1} + \phi_2 k_{s2}}{\phi_{hnf}}\right) + 2k_f - (\phi_1 k_{s1} + \phi_2 k_{s2}) + \phi_{hnf k_f}}$
Electrical Conductivity	$\frac{\sigma_{nf}}{\sigma_f} = 1 + \frac{3\left(\frac{\sigma_s}{\sigma_f} - 1\right)\phi_1}{\left(\frac{\sigma_s}{\sigma_f} + 2\right) - \left(\frac{\sigma_s}{\sigma_f} - 1\right)\phi_1}$	$\frac{\sigma_{hnf}}{\sigma_f} = 1 + \frac{3\left(\frac{\phi_1\sigma_{s1} + \phi_2\sigma_{s2}}{\sigma_f} - \phi_{hnf}\right)}{\left(\frac{\phi_1\sigma_{s1} + \phi_2\sigma_{s2}}{\phi_{hnf}\sigma_f} + 2\right) - \left(\frac{\phi_1\sigma_{s1} + \phi_2\sigma_{s2}}{\sigma_f} - \phi_{hnf}\right)}$

Table 2. Thermophysical Traits of Ag, Fe_3O_4 and H_2O [25]

Nanoparticles	$\rho(kgm^{-3})$	$C_p(Jkg^{-1}K^{-1})$	$k(Wm^{-1}K^{-1})$	$\sigma(sm^{-1})$
Argentum (Ag)	10500	235	429	6.3×10^7
Magnetite (Fe_3O_4)	5180	670	9.7	12.7
H_2O	997.1	4179	0.613	5.5×10^{-6}

This paper focuses on key physical parameters, specifically skin friction C_f and the Nusselt number Nu_x, expressed as follows:

$$C_f = \frac{\mu_{hnf}}{\rho_f u_w{}^2}\left(\frac{\partial u}{\partial y}\right)_{y=0}, \qquad Nu_x = \frac{Lq_w}{k_f(T_w - T_\infty)}, \qquad q_w = -k_{hnf}\left(\frac{\partial T}{\partial y}\right)_{y=0}, \tag{10}$$

where q_w reflects the surface heat flux. By incorporating Eq. (5) into Eq. (10), the derived formulas are as follows:

$$\sqrt{2Re_x}C_f = \frac{\mu_{hnf}}{\mu_f}f''(0), \qquad \sqrt{2/Re_x}Nu_x = -\frac{k_{hnf}}{k_f}\theta'(0), \tag{11}$$

where $Re_x = u_w L/v_f$ indicates the local Reynolds number.

3. RESULTS AND DISCUSSION

The numerical solution of the boundary-layer problem is carried out using the bvp4c function in MATLAB, which is designed to handle systems of nonlinear ordinary differential equations. The original governing partial differential equations are first reduced to similarity-based ordinary differential equations together with the relevant boundary conditions. The bvp4c function then employs a fourth-order collocation technique to generate reliable and convergent solutions. This numerical strategy enables a thorough examination of the velocity and temperature distributions and supports an in-depth evaluation of the flow behavior under different control parameters. Table 3 presents a comparative analysis of the numerical values for the conventional fluid obtained using two different computational techniques. The present study employed the bvp4c function in MATLAB, whereas Nadeem et al. [26] utilized the shooting technique. The comparison is made for various values of the parameter Pr and c. The results demonstrate excellent agreement between the two methods, with the values computed in the present study closely matching those reported by Nadeem et al. [26]. The numerical findings are further verified by comparison with Waseem et al. [27], who also

utilized the bvp4c approach, indicating the correctness of the relative error tolerance used in this study. This strong correlation validates the accuracy and reliability of the bvp4c approach for solving boundary-value problems in fluid flow and heat transfer.

Table 3. Comparison Values of $\theta'(0)$ for $\phi_1 = \phi_2 = 0$

Pr	c	Nadeem et al. [26]	Waseem et al. [27]	Present
1	-1.5	0.377412	–	0.377412510
	0	–0.549646	–0.5498508	–0.549643756
	1	–0.954786	–0.9548520	–0.954782709
	3	–1.560295	–1.5602958	–1.560295513
5	-1.5	1.3532405	–	1.353240566
	0	–1.521240	–1.5212312	–1.521239012
	1	–2.500135	–2.5001224	–2.500131408
	3	–3.886555	–3.8865480	–3.886555145

The computed values of $f''(0)$ and $-\theta'(0)$ in Table 4 illustrate the influence of s, M, c, $\Upsilon_1, \chi_1, \phi_1, \phi_1$ and Ec, while maintaining $Pr = 6.2$ and $\lambda = 1$. The results reveal that an increase in the suction parameter s leads to a significant rise in skin friction magnitude $\|f''(0)\|$, indicating stronger resistance at the wall due to the enhanced suction effect. Since $f''(0)$ is negative, a higher magnitude implies a more pronounced opposing force acting against the fluid flow, increasing the shear stress at the surface. This effect occurs because suction removes fluid from the boundary layer, reducing its thickness and intensifying velocity gradients near the wall, thereby amplifying frictional forces. Moreover, the enhancement of suction also promotes greater heat transfer efficiency, as reflected by the increasing values of $-\theta'(0)$. This suggests that as s increases, the temperature gradient at the wall becomes steeper, allowing more effective thermal energy dissipation. The reduction in boundary layer thickness due to suction minimises thermal resistance, enabling heat to be transferred more efficiently from the surface to the fluid.

The influence of the magnetic parameter M in Table 4 demonstrates that as M increases, the magnitude of $f''(0)$ decreases. Since the values of $f''(0)$ are negative, this indicates a reduction in the resistive forces acting on the fluid. This is consistent with the presence of the Lorentz force, which opposes the motion of the fluid and slows down its movement, leading to a reduction in surface shear stress. Similarly, the temperature exponent parameter c shows a slight influence on the heat transfer rate, where increasing c leads to a decrease in $-\theta'(0)$. This implies that the temperature gradient at the surface becomes less steep, slightly reducing the heat transfer efficiency.

Additionally, the presence of velocity slip Υ_1 significantly impacts the skin friction. Higher slip conditions result in lower interaction between the fluid and the surface, reducing the frictional force, which is reflected by the reduced magnitude of $f''(0)$. In physical terms, this means that with increasing slip, the fluid experiences less resistance from the surface, which weakens the opposing shear stress and contributes to a smoother flow behaviour. However, thermal slip χ_1 does not influence the skin friction coefficient $f''(0)$, as its values remain unchanged for different values of $\chi_1 = 1.0, 1.3, 1.5$. This implies that the thermal slip condition primarily affects the heat transfer characteristics rather than the momentum boundary layer. In physical terms, thermal slip alters the way heat is conducted at the wall but does not change the interaction between the fluid and the surface in terms of shear stress, leading to no effect on skin friction. The results show that increasing χ_1 decelerates the heat transfer rate, as observed from the decreasing values of $-\theta'(0)$. This occurs because thermal slip weakens the heat exchange between the surface and the fluid, reducing the thermal conductivity effect near the boundary.

Moreover, the addition of the nanoparticles concentration, specifically argentum ϕ_1, enhances the heat transfer rate and $\|f''(0)\|$. However, the addition of the magnetite nanoparticles concentration ϕ_2 exhibits a contrasting behaviour. As ϕ_2 increases, the magnitude of $f''(0)$ reduces, indicating a decrease in shear stress at the surface, while the heat transfer rate does not exhibit the same level of enhancement observed with ϕ_1. This reverse effect proposes that the thermophysical properties of magnetite nanoparticles influence the boundary layer differently compared to argentum nanoparticles, possibly due to variations in thermal conductivity, specific heat, and nanoparticle-fluid interaction, which ultimately impact the heat transfer characteristics in a distinct manner. Lastly, the Eckert number Ec, which represents the effect of viscous dissipation, influences the thermal boundary layer, where increasing Ec results in a decrease in $-\theta'(0)$, indicating a reduction in heat transfer efficiency due to internal heat generation.

Table 4. Reduced Skin Friction $f''(0)$ and Nusselt Number $-\theta'(0)$ for Various s, M, c, $\Upsilon_1, \chi_1, \phi_1, \phi_2$ and Ec when $Pr = 6.2$ and $\lambda = 1$.

s	M	c	Υ_1	χ_1	ϕ_1	ϕ_2	Ec	$f''(0)$	$-\theta'(0)$
2.5	0.2	1	0.2	0.5	0.01	0.01	0.2	-2.540893	1.687501
2.7	-	-	-	-	-	-	-	-2.627869	1.707239
3.0	-	-	-	-	-	-	-	-2.748654	1.733034
-	0.4	-	-	-	-	-	-	-2.736320	1.733011
-	0.6	-	-	-	-	-	-	-2.723602	1.733992
2.5	0.2	1.5	0.2	0.5	0.01	0.01	0.2	-2.540893	1.689150
-	-	2.0	-	-	-	-	-	-2.540893	1.690776
-	-	2.5	-	-	-	-	-	-2.540893	1.692377
2.5	0.2	1	0.3	0.5	0.01	0.01	0.2	-2.017617	1.717259
-	-	-	0.5	-	-	-	-	-1.432447	1.742948
-	-	-	0.7	-	-	-	-	-1.111681	1.753465
2.5	0.2	1	0.2	1.0	0.01	0.01	0.2	-2.540893	0.894587
-	-	-	-	1.3	-	-	-	-2.540893	0.697847
-	-	-	-	1.5	-	-	-	-2.540893	0.608615
2.5	0.2	1	0.2	0.5	0.02	0.01	0.2	-2.989177	1.693287
-	-	-	-	-	0.05	-	-	-3.651287	1.716562
-	-	-	-	-	0.07	-	-	-3.866201	1.728154
2.5	0.2	1	0.2	0.5	0.01	0.03	0.2	-2.527415	1.671212
-	-	-	-	-	-	0.05	-	-2.510901	1.654469
-	-	-	-	-	-	0.07	-	-2.491444	1.637235
2.5	0.2	1	0.2	0.5	0.01	0.01	0.5	-2.540893	1.559714
-	-	-	-	-	-	-	0.8	-2.540893	1.431928

Fig. 2 demonstrates the variation of the dimensionless temperature profile for Ag-Fe_3O_4 hybrid nanofluid, Ag nanofluid, and Fe_3O_4 nanofluid. The results reveal that the hybrid nanofluid (black line) exhibits the smallest thermal boundary layer thickness compared to single-component Ag and Fe_3O_4 nanofluids due to its superior thermal conductivity, enhanced thermal diffusivity, and increased nanoparticle interactions. The combination of argentum and magnetite nanoparticles creates a synergistic effect that improves heat transfer efficiency by promoting stronger micro-convection, reducing resistance to heat flow, and establishing a steeper temperature gradient near the heated surface. As a result, heat is dissipated more effectively, leading to a thinner thermal boundary layer, which signifies improved convective heat transfer performance in the hybrid nanofluid.

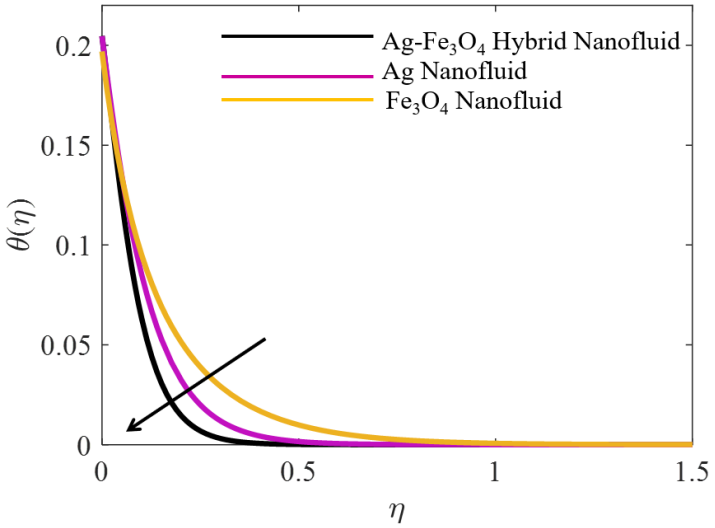

Figure 2. Nusselt Number Graph Trend for Single and Hybrid Nanofluid

Fig. 3 and Fig. 4 portray the impact of the velocity slip parameter on the velocity and temperature profiles, respectively. As observed in Fig. 3, an increase in Υ_1 exhibits an increase in the velocity profile, indicating that the fluid experiences less resistance near the surface due to the slip condition, allowing for a higher velocity within the boundary layer. This is because a larger slip parameter reduces the shear stress at the wall, leading to a more pronounced velocity gradient. Meanwhile, Fig. 4 shows that a higher slip parameter results in a lower temperature profile, thereby reducing the thermal boundary layer thickness. This

behaviour is due to the weakened heat transfer from the surface to the fluid, as slip conditions reduce the convective heat transport efficiency. Additionally, the presence of dual solutions in both figures indicates multiple steady-state behaviours for certain parameter ranges.

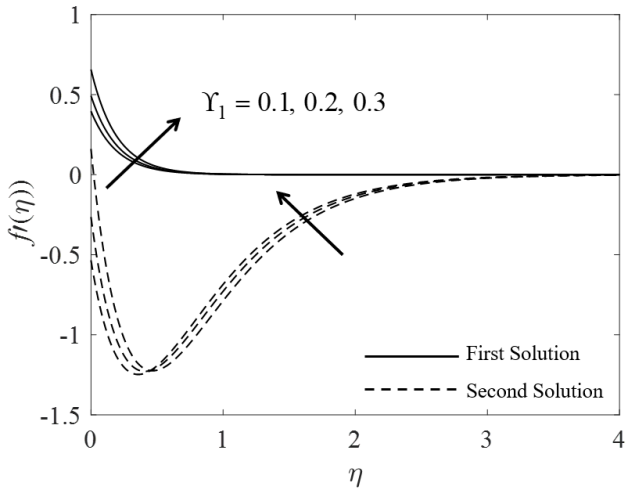

Figure 3. Velocity Profiles Distribution for Some Υ_1 Values

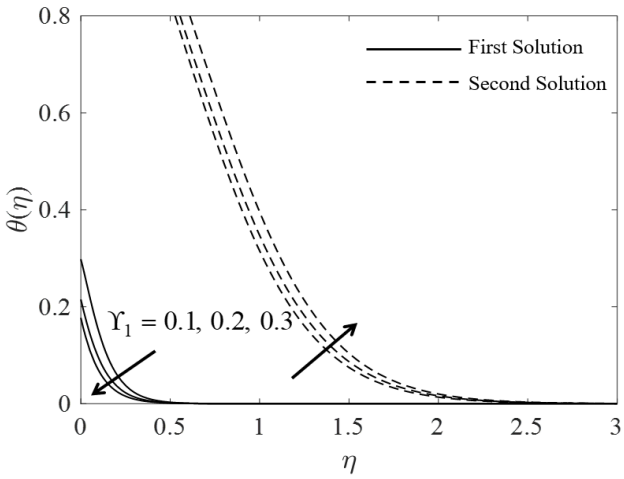

Figure 4. Temperature Profiles Distribution for Some Υ_1 Values

As shown in Fig. 5, both solutions indicate that increasing thermal slip lowers the temperature of the hybrid nanofluid. Physically, thermal slip is a condition in which there is partial resistance to heat transfer at the solid-fluid interface, meaning the fluid does not fully adhere to the surface temperature. As χ_1 increases, the ability of the fluid to absorb heat from the surface diminishes, resulting in a lower temperature distribution within the fluid. Consequently, the thermal boundary layer becomes thinner, as less heat is diffused into the nanofluid.

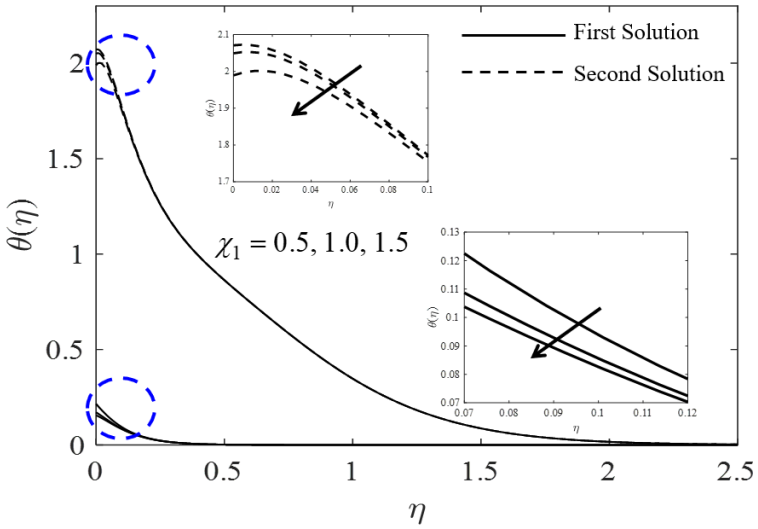

Figure 5. Temperature Profiles Distribution for Some χ_1 Values

Fig. 6 and Fig. 7 demonstrate how the velocity and temperature profiles respond to variations in the magnetic parameter. In particular, Fig. 6 reveals that as *M* rises, the velocity profile decreases, resulting in a thinner momentum boundary layer. This occurs because an increasing magnetic field generates a stronger Lorentz force, which acts as a resistive force opposing the fluid's motion. The generated Lorentz force increases drag, thereby decreasing velocity [28]. Consequently, the momentum boundary-layer thickness is reduced. The present velocity profile behavior agrees well with the findings of Aldhafeeri [29]. On the other hand, Fig. 7 shows that as *M* increases, the temperature profile rises, leading to a thicker thermal boundary layer. This behaviour is attributed to the conversion of kinetic energy into thermal energy due to the resistive effects of the Lorentz force. Opposition to fluid motion increases internal energy dissipation, raising the fluid's temperature and expanding the thermal boundary layer. The contrasting trends between the first and second solutions in both figures arise due to the nature of the solutions themselves. The first solution represents a stable physical state, while the second solution is generally associated with an unstable regime.

In accordance with standard temporal stability analysis, the first solution corresponds to a physically stable flow state characterized by decaying perturbations, whereas the second solution is unstable due to the amplification of small disturbances[30], [31].

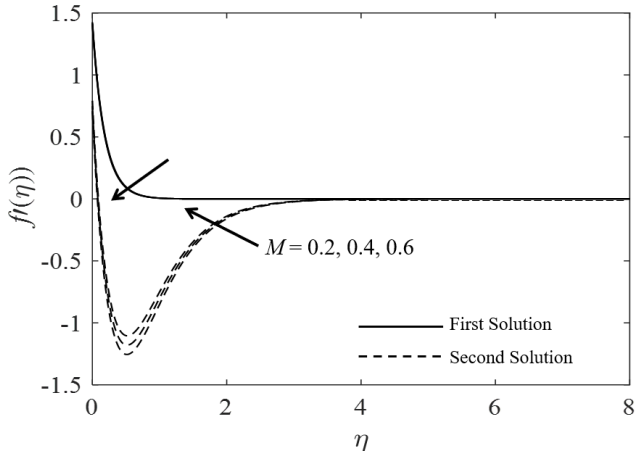

Figure 6. Velocity Profiles Distribution for Some M Values

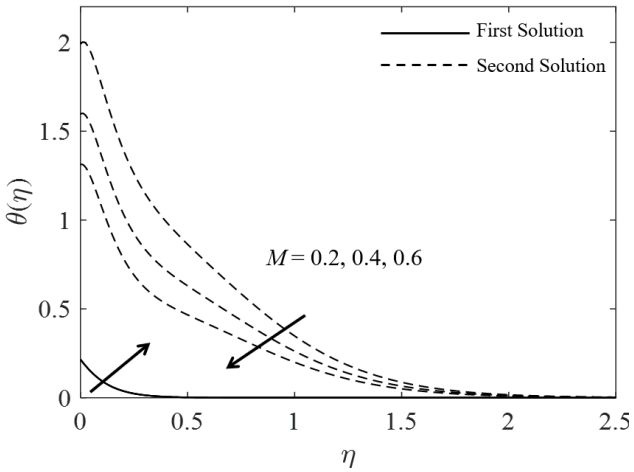

Figure 7. Temperature Profiles Distribution for Some M Values

Next, Fig. 8 highlights the impact of Eckert number variations on the behaviour of the temperature profiles, revealing that an increase in Ec causes a temperature rise in the hybrid nanofluid. Since the Eckert number quantifies viscous dissipation, it represents the conversion of kinetic energy into heat due to internal friction. As Ec increases, this effect becomes more dominant, contributing to higher heat generation. This leads to an elevated temperature distribution and a more extensive thermal boundary layer. Besides, viscous dissipation also promotes the kinetic-to-thermal energy transfer, as discussed by Chouhan et al. [32].

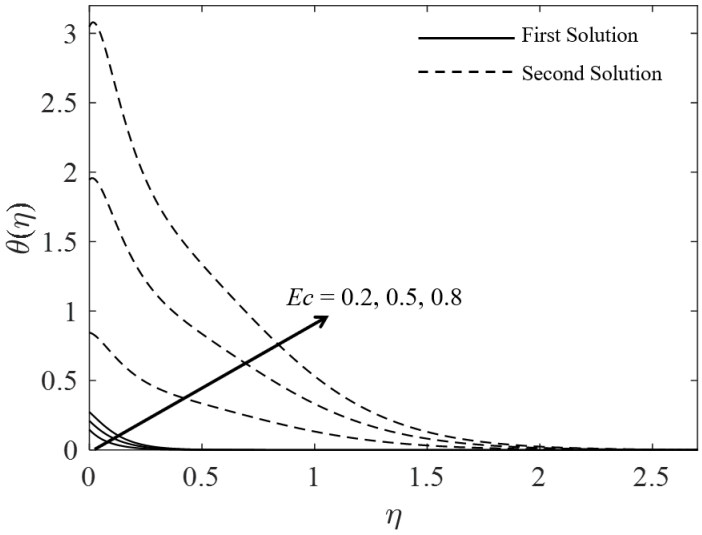

Figure 8. Temperature Profiles Distribution for Some Ec Values

Fig. 9 and Fig.10 illustrate the effects of surface contraction $(\lambda < 0)$ and surface elongation $(\lambda > 0)$ on velocity and temperature profiles. When the surface is elongated, the fluid experiences a stretching motion that enhances the velocity profile, leading to an increase in momentum transport and a thicker boundary layer, as shown in Fig. 9. This stretching effect induces a favourable pressure gradient, reducing resistance to flow and facilitating fluid motion. In Fig. 10, both positive and negative values of λ result in an increase in temperature, though the underlying mechanisms differ. For an elongated surface $(\lambda > 0)$, the stretching motion enhances fluid velocity, leading to greater shear effects and increased viscous dissipation, which generates heat within the fluid. Although elongation generally promotes convective cooling by improving heat transfer away from the surface, the localised heating effect due to viscous dissipation still contributes to a rise in temperature near the boundary layer. On the other hand, for a contracting surface $(\lambda < 0)$, a reverse flow near the wall is induced, causing the fluid velocity to attain negative values within the boundary layer. The inward motion compresses the fluid, further intensifying viscous heating and restricting convective

cooling. This compression effect traps thermal energy within the boundary layer, leading to a thicker thermal region. Consequently, despite the opposite flow behaviours, both elongation and contraction contribute to a higher temperature profile due to the dominance of viscous dissipation and heat accumulation within the thermal boundary layer.

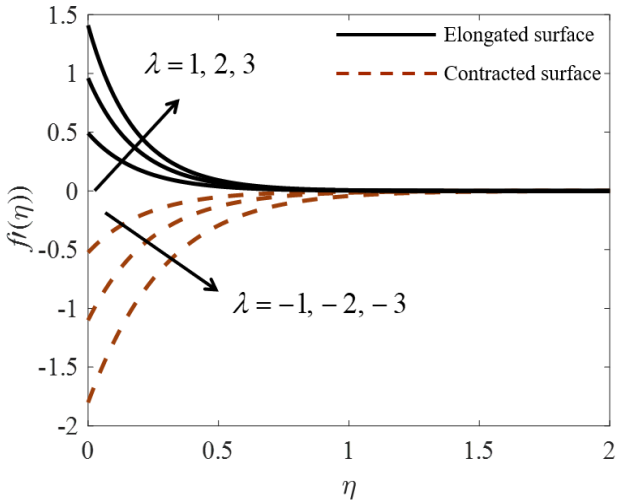

Figure 9. Velocity Profiles Distribution for Elongated/Contracted Surface

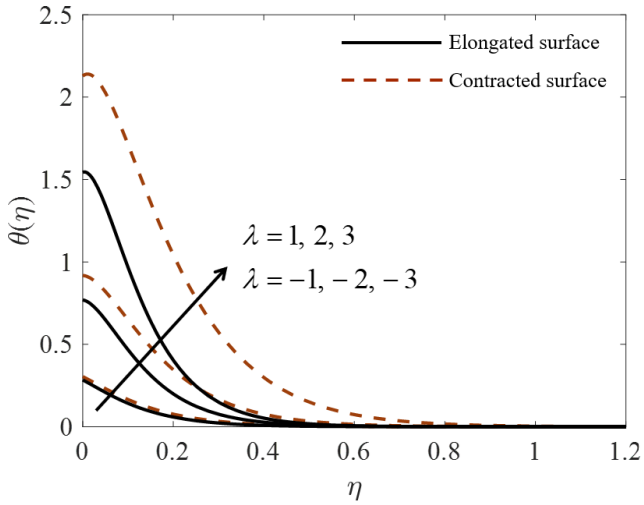

Figure 10. Temperature Profiles Distribution for Elongated/Contracted Surface

4. CONCLUSION

The flow and thermal characteristics of Ag-Fe_3O_4 hybrid nanofluid were analysed under the effects of magnetohydrodynamics, viscous dissipation, velocity slip, thermal slip, and surface deformation. The study found that an increasing magnetic field slows the fluid due to the Lorentz force while elevating its temperature, leading to a thicker thermal boundary layer. Higher viscous dissipation intensifies heat accumulation, further enhancing the temperature distribution. Surface elongation improves convective heat transfer by promoting fluid motion, while contraction suppresses it, causing greater thermal resistance and heat buildup. The presence of velocity slip weakens momentum exchange near the surface, reducing the effectiveness of flow acceleration, whereas thermal slip limits the heat transfer rate, resulting in lower surface heat flux. These findings underscore the relevance of Ag-Fe_3O_4 hybrid nanofluid in advanced thermal management applications, particularly in enhancing energy-efficient cooling systems, biomedical devices, and industrial heat transfer processes. A deeper understanding of these factors enables the refinement of nanofluid technologies, optimising their performance for industrial and engineering applications.

Author Contributions

Rahimah Jusoh: Conceptualization, Formal Analysis. Zulkhibri Ismail: Data curation, Investigation. Mikhail Sheremet: Methodology, Validation. Nooraini Zainuddin: Visualization. Mohd Hisyam Ariff: Writing-Review and Editing. All authors discussed the results and contributed to the final manuscript.

Funding Statement

This research was financially supported by Universiti Malaysia Pahang Al-Sultan Abdullah through research grant RDU223202, which significantly contributed to the completion of this study.

Acknowledgment

The authors would like to express their sincere gratitude to Universiti Malaysia Pahang Al-Sultan Abdullah for the financial assistance, facilities, and continuous support provided.

Declarations

The authors confirm that no conflicts of interest are associated with this article.

Declaration of Generative AI and AI-assisted technologies

Generative AI tools (e.g., ChatGPT) were used solely for language refinement (grammar, spelling, and clarity). The scientific content, analysis, interpretation, and conclusions were developed entirely by the authors. The authors reviewed and approved all final text.

REFERENCES

[1] S. U. S. Choi and J. A. Eastman, "ENHANCING THERMAL CONDUCTIVITY OF FLUIDS WITH NANOPARTICLES," in *The Proceedings of the 1995 ASME International Mechanical Engineering Congress and Exposition*, San Francisco, USA, 1995, pp. 99–105, doi: https://doi.org/10.1115/IMECE1995-0926

[2] R. Zhang, N. Xu, X. Cao, C. Wei, S. Qing, and Y. He, "SHAPE-DEPENDENT THERMAL AND FLUIDIC PROPERTIES OF AG-H2O NANOFLUIDS IN MICROCHANNEL: A MOLECULAR DYNAMICS STUDY," *Chem. Phys.*, vol. 595, Jul. 2025, doi: https://doi.org/10.1016/j.chemphys.2025.112726

[3] D. F. Heravi, H. R. Goshayeshi, and R. Saleh, "ENHANCING EFFICIENCY OF A LABORATORY-SCALE HYBRID COOLING TOWER USING FE3O4-WATER NANOFLUID AND SPIRAL COILS," *Heliyon*, vol. 11, no. 1, p. e41370, Jan. 2025, doi: https://doi.org/10.1016/j.heliyon.2024.e41370

[4] Y. Lin *et al.*, "PRABHAKAR FRACTIONAL SIMULATION FOR THERMAL AND SOLUTAL TRANSPORT ANALYSIS OF A CASSON HYBRID NANOFLUID FLOW OVER A CHANNEL WITH BUOYANCY EFFECTS," *J. Magn. Magn. Mater.*, vol. 586, Nov. 2023, doi: https://doi.org/10.1016/j.jmmm.2023.171176

[5] A. K. Hussein *et al.*, "A REVIEW OF THE APPLICATION OF HYBRID NANOFLUIDS IN SOLAR STILL ENERGY SYSTEMS AND GUIDELINES FOR FUTURE PROSPECTS,", *Elsevier Ltd*, Apr. 01, 2024, doi: https://doi.org/10.1016/j.solener.2024.112485

[6] L. S. Sundar, S. M. O. Tavares, A. M. B. Pereira, and A. C. M. Sousa, "REVIEW ON THERMAL EFFICIENCY AUGMENT OF FLAT PLATE COLLECTOR EQUIPPED WITH MONO AND HYBRID NANOFLUIDS AND WITH INSERTS,", *Elsevier B.V*, Mar. 01, 2025, doi: https://doi.org/10.1016/j.ijft.2025.101111

[7] R. Turcu *et al.*, "NEW POLYPYRROLE-MULTIWALL CARBON NANOTUBES HYBRID MATERIALS," *Journal of Optoelectronics and Advanced Materials*, vol. 8, no. 2, pp. 643–647, 2006.

[8] M. Asim and F. R. Siddiqui, "HYBRID NANOFLUIDS—NEXT-GENERATION FLUIDS FOR SPRAY-COOLING-BASED THERMAL MANAGEMENT OF HIGH-HEAT-FLUX DEVICES," *MDPI*, Feb. 01, 2022, doi: https://doi.org/10.3390/nano12030507

[9] M. Rafid *et al.*, "AUGMENTATION OF HEAT EXCHANGER PERFORMANCE WITH HYBRID NANOFLUIDS: IDENTIFYING RESEARCH GAPS AND FUTURE INDICATIONS - A REVIEW," *Elsevier Ltd.*, Jun. 01, 2024, doi: https://doi.org/10.1016/j.icheatmasstransfer.2024.107537

[10] D. Madhesh and S. Kalaiselvam, "EXPERIMENTAL ANALYSIS OF HYBRID NANOFLUID AS A COOLANT," in *Procedia Engineering*, Elsevier Ltd, 2014, pp. 1667–1675, doi: https://doi.org/10.1016/j.proeng.2014.12.317

[11] A. Hyder, Y. J. Lim, I. Khan, and S. Shafie, "INVESTIGATING HEAT TRANSFER CHARACTERISTICS IN NANOFLUID AND HYBRID NANOFLUID ACROSS MELTING STRETCHING/SHRINKING BOUNDARIES," *Bionanoscience*, vol. 14, no. 2, pp. 1181–1195, Jun. 2024, doi: https://doi.org/10.1007/s12668-024-01309-z

[12] R. Wang *et al.*, "A REVIEW ON SLIP BOUNDARY CONDITIONS AT THE NANOSCALE: RECENT DEVELOPMENT AND APPLICATIONS," *Beilstein Journal of Nanotechnology*, vol. 12, pp. 1237–1251, 2021, doi: https://doi.org/10.3762/bjnano.12.91

[13] V. K. Patel, J. U. Pandya, and M. R. Patel, "TESTING THE INFLUENCE OF TIO2− AG/WATER ON HYBRID NANOFLUID MHD FLOW WITH EFFECT OF RADIATION AND SLIP CONDITIONS OVER EXPONENTIALLY STRETCHING & SHRINKING SHEETS," *J. Magn. Magn. Mater.*, vol. 572, no. 170591, pp. 1–14, Apr. 2023, doi: https://doi.org/10.1016/j.jmmm.2023.170591

[14] P. M. Patil, B. Goudar, and E. Momoniat, "CASSON-WILLIAMSON TERNARY HYBRID NANOFLUID FLOW OVER A YAWED CYLINDER WITH THE IMPACTS OF MULTIPLE SLIPS," *Int. J. Numer. Methods Heat Fluid Flow*, Nov. 2024, doi: https://doi.org/10.1108/HFF-03-2024-0176

[15] E. Ragulkumar, G. Palani, P. Sambath, and A. J. Chamkha, "DISSIPATIVE MHD FREE CONVECTIVE NANOFLUID FLOW PAST A VERTICAL CONE UNDER RADIATIVE CHEMICAL REACTION WITH MASS FLUX," *Sci. Rep.*, vol. 13, no. 1, Dec. 2023, doi: https://doi.org/10.1038/s41598-023-28702-0

[16] Md. A. K. Azad, Md. Hasanuzzaman, Md. M. Hossain, and A. Miyara, "SUCTION AND LORENTZ FORCE EFFECTS ON MHD FREE CONVECTIVE TRANSPORT OF MICROPOLAR FLUID PASSING A UNSTEADY ANALYSIS," *Alexandria Engineering Journal*, vol. 100, pp. 72–81, Aug. 2024, doi: https://doi.org/10.1016/j.aej.2024.04.067

[17] Q. Raza, R. Younus, H. A. Ghazwani, and A. J. Chamkha, "AN EMPIRICAL ANALYSIS OF HYBRID MHD FERROFLUID UNSTEADY FLOW OF TWO-DIMENSIONAL HEAT TRANSFER ACROSS A POROUS CHANNEL," *Numeri. Heat Transf. A Appl.*, pp. 1–23, Jul. 2024, doi: https://doi.org/10.1080/10407782.2024.2382911

[18] A. Naseem and A. Ghafoor Kasana, "NUMERICAL ASSESSMENT OF MHD HYBRID NANOFLUID FLOW OVER AN EXPONENTIALLY STRETCHING SURFACE IN THE PRESENCE OF MIXED CONVECTION AND NON UNIFORM HEAT SOURCE/SINK," *Results in Engineering*, vol. 22, Jun. 2024, doi: https://doi.org/10.1016/j.rineng.2024.102294

[19] S. Del Giudice, C. Nonino, and S. Savino, "EFFECTS OF VISCOUS DISSIPATION AND TEMPERATURE DEPENDENT VISCOSITY IN THERMALLY AND SIMULTANEOUSLY DEVELOPING LAMINAR FLOWS IN MICROCHANNELS," *Int. J. Heat Fluid Flow*, vol. 28, no. 1, pp. 15–27, 2007, doi: https://doi.org/10.1016/j.ijheatfluidflow.2006.05.007

[20] I. Waini, S. Alabdulhady, A. Ishak, and I. Pop, "VISCOUS DISSIPATION EFFECTS ON HYBRID NANOFLUID FLOW OVER A NON-LINEARLY SHRINKING SHEET WITH POWER-LAW VELOCITY," *Heliyon*, vol. 9, no. 10, Oct. 2023, doi: https://doi.org/10.1016/j.heliyon.2023.e20910

[21] S. V. Padma, M. P. Mallesh, M. Sanjalee, and A. J. Chamkha, "FLOW STABILITY SIMULATION OVER A STRETCHING/SHRINKING SURFACE WITH THERMAL RADIATION AND VISCOUS DISSIPATION OF HYBRID NANOFLUIDS," *J. Therm. Anal. Calorim.*, vol. 149, no. 6, pp. 2749–2763, Mar. 2024, doi: https://doi.org/10.1007/s10973-023-12858-y

[22] A. Ishak, "MHD BOUNDARY LAYER FLOW DUE TO AN EXPONENTIALLY STRETCHING SHEET WITH RADIATION EFFECT," *Sains Malays.*, vol. 40, no. 4, pp. 391–395, 2011.

[23] B. Takabi and S. Salehi, "AUGMENTATION OF THE HEAT TRANSFER PERFORMANCE OF A SINUSOIDAL CORRUGATED ENCLOSURE BY EMPLOYING HYBRID NANOFLUID," *Advances in Mechanical Engineering*, vol. 2014, no. 147059, pp. 1–16, 2014, doi: https://doi.org/10.1155/2014/147059

[24] S. Hussain, S. E. Ahmed, and T. Akbar, "ENTROPY GENERATION ANALYSIS IN MHD MIXED CONVECTION OF HYBRID NANOFLUID IN AN OPEN CAVITY WITH A HORIZONTAL CHANNEL CONTAINING AN ADIABATIC OBSTACLE," *Int. J. Heat Mass Transf.*, vol. 114, pp. 1054–1066, 2017, doi: https://doi.org/10.1016/j.ijheatmasstransfer.2017.06.135

[25] A. Gul, I. Khan, and S. Shafie, "ENERGY TRANSFER IN MIXED CONVECTION MHD FLOW OF NANOFLUID CONTAINING DIFFERENT SHAPES OF NANOPARTICLES IN A CHANNEL FILLED WITH SATURATED POROUS MEDIUM," in *Nanofluid Heat and Mass Transfer in Engineering Problems*, InTech, 2017, doi: https://doi.org/10.5772/67367

[26] S. Nadeem, R. Ul Haq, and Z. H. Khan, "HEAT TRANSFER ANALYSIS OF WATER-BASED NANOFLUID OVER AN EXPONENTIALLY STRETCHING SHEET," *Alexandria Engineering Journal*, vol. 53, no. 1, pp. 219–224, 2014, doi: https://doi.org/10.1016/j.aej.2013.11.003

[27] M. Waseem, W. H. Hassan, M. Jawad, G. Bognár, and R. Ghodhbani, "EXAMINATION OF CHEMICAL REACTION ON SECOND-GRADE NANOFLUID AND MICROPOLAR NANOFLUID DUE TO EXPONENTIAL STRETCHABLE SHEET: A COMPARATIVE STUDY," *S. Afr. J. Chem. Eng.*, vol. 53, pp. 373–385, Jul. 2025, doi: https://doi.org/10.1016/j.sajce.2025.05.010

[28] S. Panda, MD. Shamshuddin, A. M. Obalalu, S. O. Salawu, and S. R. Mishra, "CATTANEO-CHRISTOV HYPOTHESIS IN A MICROPOLAR NANOFLUID FLOW OVER A STRETCHING SHEET SUBJECTED TO EXPONENTIAL SPACE-BASED HEAT GENERATION AND BILATERAL REACTIONS," *Case Studies in Thermal Engineering*, vol. 74, p. 106813, Oct. 2025, doi: https://doi.org/10.1016/j.csite.2025.106813

[29] A. A. Aldhafeeri, "A NUMERICAL ANALYSIS OF THE RADIATIVE BLOOD-BASED HYBRID NANOFLUID FLOW OVER AN EXPONENTIALLY EXTENDING HEATED SURFACE USING A POROUS MEDIUM," *J. Radiat. Res. Appl. Sci.*, vol. 18, no. 2, p. 101503, Jun. 2025, doi: https://doi.org/10.1016/j.jrras.2025.101503

[30] N. A. Zainal, R. Nazar, H. A. Zuberi, and I. Pop, "ENHANCED HEAT TRANSFER IN HYBRID NANOFLUID: ROLE OF SUCTION AND WEDGE ANGLE ON BOUNDARY LAYER DYNAMICS," *Journal of Quality Measurement and Analysis*, vol. 21, no. 2, pp. 163–174, Jun. 2025, doi: https://doi.org/10.17576/jqma.2102.2025.12

[31] N. A. Zainal, R. Nazar, K. Naganthran, and I. Pop, "STABILITY ANALYSIS OF UNSTEADY MHD REAR STAGNATION POINT FLOW OF HYBRID NANOFLUID," *Mathematics*, vol. 9, no. 19, Oct. 2021, doi: https://doi.org/10.3390/math9192428

[32] N. Chouhan, R. Jain, K. Loganathan, and S. Eswaramoorthi, "HEAT AND MASS TRANSMISSION IN MAXWELL NANOFLUID FLOW OVER AN EXPONENTIAL STRETCHABLE SURFACE WITH SWIMMING OF MOTILE GYROTACTIC MICROORGANISMS," *International Journal of Thermofluids*, vol. 30, Nov. 2025, doi: https://doi.org/10.1016/j.ijft.2025.101466